molecules

MDPI

Article

Phytochemical Profiling and Exploratory Evaluation of *Momordica charantia* in a Cadmium-Induced Murine Model of Splenic Injury

Jeancy Moke Boy [1], Jonathan Mpoyi Mukanya [1,2], Kevin Kongolo Muamba [1], Isaac Elaka Kaba [3], Paulin Kapepula Mutwale [1], Nadège Kabamba Ngombe [1] and Dieudonné Tshitenge Tshitenge [1,4,*]

1 Centre d'Etudes des Substances Naturelles d'Origine Végétale, Faculty of Pharmaceutical Sciences, University of Kinshasa, Kinshasa XI B.P. 212, Kinshasa, Democratic Republic of the Congo
2 Center for Chemico- and Biomedicinal Research, Department of Chemistry, Faculty of Sciences, Rhodes University, Grahamstown P.O. Box 94, Eastern Cape, South Africa
3 Department of Chemistry, College of Chemistry, University of California, Berkeley, Berkeley, CA 94720-1460, USA
4 Crop Protection, Research & Development, Crop Science Division, Bayer AG, 40789 Monheim am Rhein, Germany
* Correspondence: dtshitenge2007@yahoo.com or dieudonne.tshitenge@bayer.com

Abstract

Momordica charantia L. is traditionally used for the management of splenomegaly, although empirical evidence supporting this ethnomedical indication remains limited. This study primarily investigated the traditional fresh leaf/stem infusion and, comparatively, related *M. charantia* preparations in a cadmium chloride ($CdCl_2$)-induced murine model of splenic injury. Ninety-six Swiss mice were allocated to eight groups, with terminal assessments on Days 1, 7, and 9; $CdCl_2$ was administered on Day 4. Splenic outcomes included absolute and relative spleen mass and qualitative histopathology. Phytochemical profiling was performed by ultra-performance liquid chromatography coupled to high-resolution mass spectrometry (UPLC-HRMS), and radical-scavenging activity was assessed using ABTS and DPPH assays. At Day 9, the traditional fresh leaf/stem infusion showed the strongest and most consistent treatment-associated signal, with lower relative and absolute spleen masses than the $CdCl_2$-exposed disease control. Several other preparations showed numerical reductions in absolute spleen mass but did not meet multiplicity-adjusted significance thresholds. UPLC-HRMS revealed diverse features consistent with triterpenoid-, glycoside-, sterol-, and oxygenated lipid-related natural-product classes. These exploratory findings provide experimental support for further investigation of the traditional fresh leaf/stem infusion, while not establishing clinical efficacy against human splenomegaly.

Keywords: *Momordica charantia*; splenic injury; splenomegaly; triterpenoids; phytochemical profiling; UPLC-HRMS

Check for updates

Academic Editor: Dorota Wianowska

Received: 2 October 2026
Revised: 13 November 2026
Accepted: 16 November 2026
Published: 18 November 2026

Copyright: © 2026 by the authors. Licensee MDPI, Basel, Switzerland. This article is an open access article distributed under the terms and conditions of the Creative Commons Attribution (CC BY) license.

1. Introduction

Traditional plant-based medicines have been used for centuries across Africa to address a wide range of health challenges. Beyond their role in managing common infections, traditional remedies are generally affordable and have been used for the treatment of several chronic and life-threatening conditions, including splenomegaly [1,2]. Tropical splenomegaly syndrome is a common disease that is caused by chronic malaria, which accounts for up to 45% of cases in sub-Saharan Africa. Management of the underlying cause

remains the primary recommended strategy for splenomegaly. However, in chronic or incurable conditions such as liver cirrhosis, schistosomiasis, or hematological malignancies, treatment relief is often only partial, and residual splenic hypertrophy commonly persists despite intervention. In such cases, additional therapeutic options are limited. Splenectomy, while effective in reducing spleen size, carries significant risks, including post-operative infection and thrombosis, and is not always feasible in resource-limited settings [3,4]. Existing pharmacological treatments, such as antiparasitic praziquantel [5] or radiotherapy for cancer [6], can provide symptomatic relief but may be too expensive, toxic, or simply unavailable in low-income environments [7]. Thus, there is a clear and unmet need for accessible, effective, and well-tolerated therapeutic alternatives, mainly in sub-Saharan Africa, where the disease burden is highest. Given the prevalence of parasitic diseases and splenomegaly conditions in most Sub-Saharan African regions, several herbal medicines or traditional plant-based recipes have emerged as a practical and most accessible alternative treatment for populations with limited access to modern healthcare. Our ethnobotanical investigations on a traditional preparation used for management of spleen disorders led to *Momordica charantia* (bitter melon), a plant widely consumed as a vegetable and deeply embedded in Congolese traditional medicine. Despite previous research demonstrating the antioxidant, anti-inflammatory, and hepatoprotective activities of this species [8], including its safe profile [9], no study has directly assessed the therapeutic properties of *M. charantia* on any in vivo models for spleen disorders. One recent study has reported its beneficial use to treat liver disorders [10]. Here, we explore for the first time the in vivo anti-splenomegaly efficacy of a traditional preparation of *M. charantia*, along with its aqueous and organic extracts from leaves, stems, and fruits, using a murine model of chemically induced splenic injury. We further investigated the tissue integrity of mouse spleens and the histological impact of treatments with *M. charantia* using histopathology. To support botanical authenticity, raw material quality control, and future standardization, micrographic fingerprinting was performed. Furthermore, we performed exploratory UPLC-HRMS phytochemical profiling of *M. charantia* extracts to learn more about the potential of this traditional plant-based remedy for managing splenomegaly and as a promising source of new bioactive compounds.

2. Results

2.1. In Vivo Efficacy of M. charantia

From 96 scheduled animal entries, 86 provided analyzable paired body-mass and spleen-mass measurements. Ten unplanned deaths occurred, and the animals were not replaced (Table 1). Two deaths occurred by Day 1 in the dried-fruit infusion group; two by Day 7 in the dried leaf/stem infusion group; and six by Day 9 (praziquantel: $n = 2$; fresh-fruit infusion: $n = 1$; dried leaf/stem infusion: $n = 1$; leaf/stem percolate: $n = 2$). The records established neither the cause of death nor the sex of the deceased animals. The deceased animals were excluded from subsequent analyses; no spleens were collected from them, and no post-mortem histopathology was performed.

2.1.1. Evaluation of Mouse Body and Spleen Weights

Body-weight differences across the eight experimental groups are shown in Figure 1 and Table S1 (see Supporting Information). Figure 1 and Table S1 present the variation in body weight observed in mice from the start of the study to the time of euthanasia. This difference serves as an indicator for assessing the activity of *M. charantia* extracts in promoting weight gain or loss throughout the treatment period. When compared with the disease control group, i.e., mice treated with saline solution and exhibiting weight loss during the treatment period, the administration of *M. charantia* extracts led to positive mean

changes in several treatment groups in body mass at the later terminal time points; however, these observations should be interpreted cautiously given the small endpoint sample sizes.

Table 1. Relative spleen weight at each terminal sampling day (mean ± standard deviation).

Treatment	Day 1 Relative	Day 7 Relative	Day 9 Relative
Disease control (saline)	4.96 ± 0.83 (4)	6.67 ± 1.54 (4)	6.37 ± 1.12 (4)
Praziquantel	3.15 ± 0.63 (4)	6.17 ± 1.83 (4)	4.14 ± 0.45 (2)
Fresh leaf/stem infusion (the herbal preparation)	4.68 ± 1.02 (4)	6.68 ± 0.87 (4)	3.45 ± 0.78 (4)
Fresh-fruit infusion	3.71 ± 0.75 (4)	6.58 ± 1.43 (4)	4.89 ± 0.96 (3)
Dried leaf/stem infusion	5.41 ± 1.98 (4)	6.78 ± 1.51 (2)	4.94 ± 0.38 (3)
Dried-fruit infusion	4.81 ± 1.73 (2)	5.88 ± 0.75 (4)	5.41 ± 1.76 (4)
Leaf/stem percolate	3.93 ± 0.48 (4)	6.26 ± 1.89 (4)	4.49 ± 0.62 (2)
Fruit percolate	3.77 ± 1.18 (4)	6.18 ± 1.24 (4)	4.70 ± 0.86 (4)

Mean ± SD (n); relative spleen mass in mg/g body mass. Day 1 is a pre-cadmium cohort. Each value is based on surviving animals with recorded spleen and body masses. When $n = 2$ or 3, respectively, two or one scheduled animals had died before terminal sampling.

Table 2. Exploratory treatment-versus-disease-control comparisons for relative and absolute spleen mass at Days 7 and 9.

Treatment	Day 7 Relative	Day 7 Absolute	Day 9 Relative	Day 9 Absolute
Praziquantel	1.000	1.000	0.157	0.236
Fresh leaf/stem infusion (the herbal preparation)	1.000	1.000	0.048	0.041
Fresh-fruit infusion	1.000	1.000	0.299	0.236
Dried leaf/stem infusion	1.000	1.000	0.299	0.100
Dried-fruit infusion	1.000	0.304	0.401	0.236
Leaf/stem percolate	1.000	0.853	0.299	0.056
Fruit percolate	1.000	0.853	0.299	0.089

Cells show Holm-adjusted two-sided Welch p values for seven comparisons within each day/outcome family. These exploratory within-family results do not account for searching across two days and two correlated outcomes. In the pooled 28-comparison sensitivity correction, no comparison meets $p < 0.05$.

Table 3. Day-9 absolute spleen-mass outcomes and exploratory Holm-adjusted treatment-versus-disease-control comparisons.

Day-9 Treatment	Absolute Spleen Mass	Reduction vs. Control	Holm-Adjusted p
Disease control	137.28 mg	—	—
Fresh leaf/stem infusion (the herbal preparation)	72.30 mg	47.3%	0.041
Leaf/stem percolate	71.80 mg	47.7%	0.056
Praziquantel	75.45 mg	45.0%	0.236
Fresh-fruit infusion	82.00 mg	40.3%	0.236
Fruit percolate	85.35 mg	37.8%	0.089
Dried leaf/stem infusion	86.27 mg	37.2%	0.100
Dried-fruit infusion	91.47 mg	33.4%	0.236

The Day-9 data show that the traditional fresh leaf/stem infusion produced the most consistent treatment-associated signal across both relative and absolute spleen-mass outcomes. Each treatment was compared with the $CdCl_2$-exposed saline disease-control group.

On Day 7, the disease-control group had a mean relative spleen mass of 6.67 ± 1.54 mg/g ($n = 4$). Mean values for treated groups ranged from 5.88 to 6.78 mg/g, and no exploratory

treatment-versus-control comparison was significant after Holm adjustment within the Day-7 relative-mass family. Absolute spleen mass averaged 139.03 ± 19.83 mg in disease controls. Dried-fruit infusion had the lowest mean absolute mass (105.78 ± 16.58 mg; 23.9% lower than the control mean), but the exploratory comparison did not remain significant after adjustment for seven contrasts (Holm-adjusted $p = 0.304$).

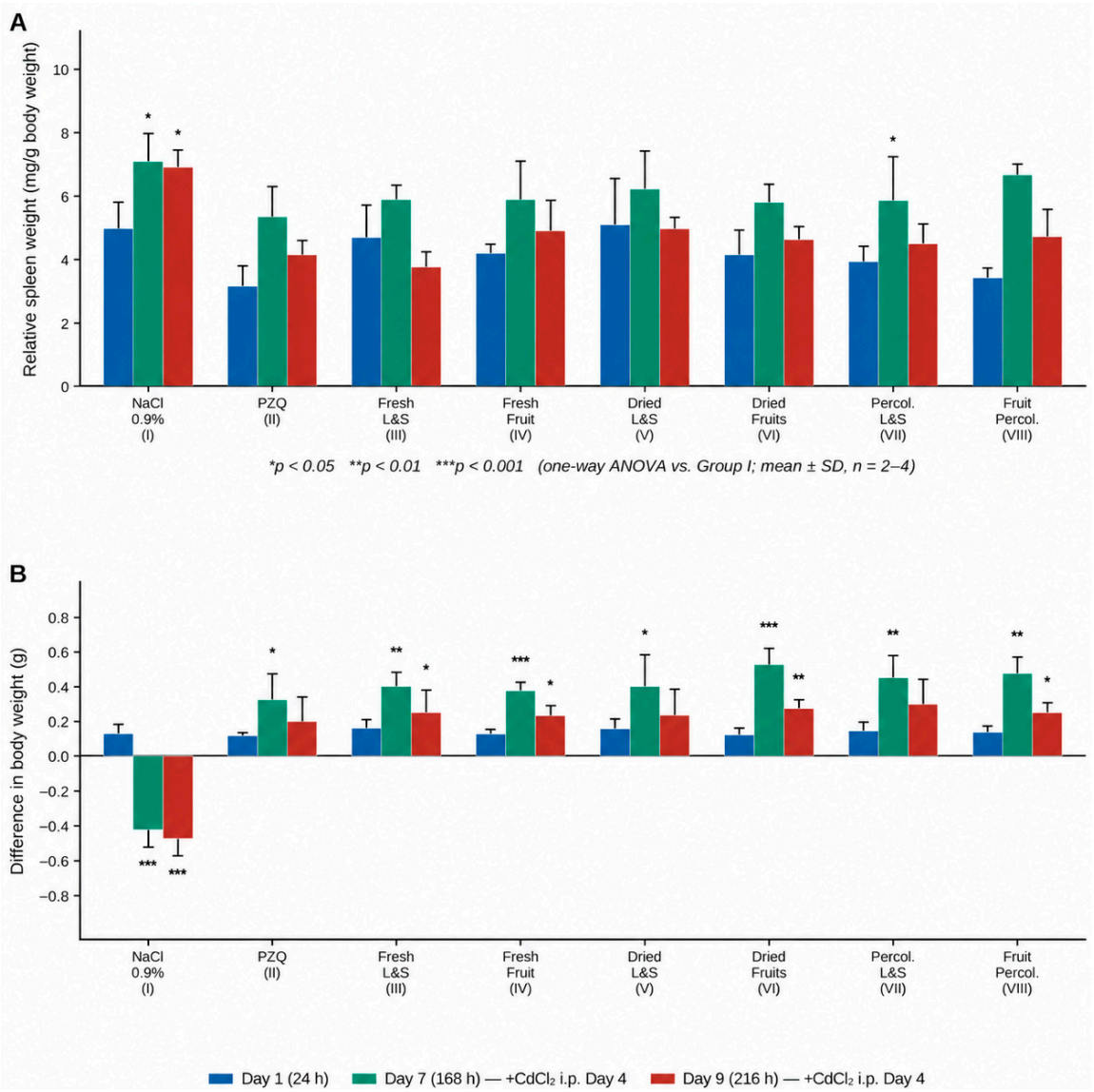


Figure 1. Effects of *Momordica charantia* extracts on relative spleen weight and body weight in a $CdCl_2$-induced murine splenomegaly model. (**A**) Relative spleen weight (mg/g body weight) and (**B**) difference in body weight (g) recorded at Day 1 (24 h), Day 7 (168 h), and Day 9 (216 h) across eight treatment groups. A single intraperitoneal injection of $CdCl_2$ (1.8 mg/kg) was administered on Day 4 to all groups. Group I: NaCl 0.9% ($CdCl_2$-exposed saline disease-control); Group II: praziquantel (300 mg/kg/12 h, orally); Group III: infusion of fresh leaves and stems (traditional healer's preparation, 300 mg dry-extract/kg/day); Group IV: infusion of fresh fruits (300 mg dry-extract/kg/day); Group V: infusion of dried leaves and stems (300 mg dry-extract/kg/day); Group VI: infusion of dried fruits (300 mg dry-extract/kg/day); Group VII: percolate of dried leaves and stems (300 mg dry-extract/kg/day); Group VIII: percolate of dried fruits (300 mg dry-extract/kg/day). All extracts were administered orally for 9 days. Data are expressed as mean ± SD (n = 2–4). Statistical significance was determined by one-way ANOVA compared to Group I: * $p < 0.05$, ** $p < 0.01$, *** $p < 0.001$.

On Day 9, mean relative spleen mass was 6.37 ± 1.12 mg/g ($n = 4$) in disease controls and 3.45 ± 0.78 mg/g ($n = 4$) in fresh leaf/stem infusion animals (45.9% lower group mean). The associated exploratory Welch comparison yielded an unadjusted $p = 0.0068$ and a seven-comparison Holm-adjusted $p = 0.0478$. Mean absolute spleen mass was likewise lower in the fresh leaf/stem group (72.30 versus 137.28 mg; 47.3% lower; unadjusted $p = 0.0059$; seven-comparison Holm-adjusted $p = 0.0414$). Terminal mean body masses were 21.00 and 21.75 g, respectively. The concordant absolute spleen-mass difference argues against an explanation based only on the body-mass denominator.

Crucially, when the entire exploratory analysis of 28 comparisons across Days 7 and 9 and both spleen outcomes was treated as a single multiplicity family, the fresh leaf/stem Day-9 comparisons were no longer statistically significant (Holm-adjusted $p = 0.1845$ for relative and 0.1655 for absolute spleen mass). Thus, the favorable Day-9 observation is sensitive to the multiplicity definition and should not be interpreted as unequivocally significant or confirmatory. At Day 7, the corresponding fresh leaf/stem and control mean relative masses were nearly identical (6.68 and 6.67 mg/g). Differences in cohort means across days cannot establish recovery within animals. A previously explored ordinary factorial ANOVA analysis did not demonstrate a treatment × sampling-day interaction (approximately $p = 0.429$). This analysis was not used as confirmatory evidence because the treatment-by-day groups were small and unequal in size (n = 2–4 owing to mortality), and the limited sample sizes did not permit reliable assessment of standard ANOVA assumptions such as residual normality and homogeneity of variance.

As reported in Tables 1–3, the traditional herbal preparation, i.e., the fresh leaf/stem infusion, showed among the tested preparations the most consistent Day-9 evidence of reduced splenic enlargement, with concordant reductions in both absolute and relative spleen mass and the strongest adjusted statistical evidence. Several other preparations, particularly the leaf/stem percolate, fruit percolate, and dried leaf/stem infusion, also showed substantial numerical reductions in absolute spleen mass, but these comparisons did not reach the multiplicity-adjusted significance threshold and should therefore be regarded as supportive trends rather than established treatment effects.

$CdCl_2$ administration was associated with increased relative spleen mass by Day 7 (Figure 1, Tables 1, 2, S1 and S2, $p < 0.05$); however, none of the exploratory treatment-versus-control comparisons reached the Holm-adjusted significance threshold. At Day 9, several treated groups showed lower mean spleen-mass values, with the traditional fresh leaf/stem infusion showing the strongest and most consistent treatment-associated signal, hinting at a beneficial effect of *M. charantia*. Cadmium exerts well-documented immunotoxic effects that disrupt both humoral and cell-mediated immunity, manifesting in rodents as thymic atrophy and progressive splenomegaly. At the intracellular level, cadmium-induced damage is mediated primarily through oxidative stress, involving excessive reactive oxygen species production, glutathione depletion, and activation of a mitochondrial caspase-dependent apoptotic pathway, collectively driving apoptosis of thymic and splenic cells [11]. Cadmium additionally inhibits mitogenic cell proliferation, induces morphological alterations in immune organs, and reduces immune cell counts in both the thymus and spleen [12]. Consistent with these mechanisms, mice in Group I exhibited progressive body weight loss alongside increasing spleen weight throughout the study period (see Supporting Information Tables S1–S3).

2.1.2. Splenic Histopathological Analysis

Histopathological examination was performed on 48 spleen samples collected on days 1, 7, and 9 (Figure 2) by an experienced histopathologist. The assessment was qualitative and performed blinded to treatment allocation. Accordingly, the histopathological observations

are interpreted descriptively and as supportive of the spleen-mass findings. The evaluation was based on expert morphological interpretation of splenic tissue architecture and pathological changes and was qualitative rather than derived from a predefined semiquantitative scoring system. Accordingly, the histopathological findings are presented as expert descriptive observations that complement the quantitative spleen-mass data. On Day 7, one case of haemorrhagic necrosis was identified, with a further isolated case observed on Day 9 (Figure 2B). Passive congestion, siderophage accumulation, and macrophage alterations, including multinucleated giant cells associated with macrophage aggregates, were also observed, particularly in the $CdCl_2$-exposed saline disease-control group, and were considered compatible with $CdCl_2$-associated splenic injury. Similar findings were present to a lesser extent in some treated animals. Overall, the histopathological pattern was consistent with more pronounced splenic alterations in the disease-control group and comparatively better preservation of tissue architecture in several treated samples. Because the assessment was qualitative, these observations should be interpreted as supportive morphological evidence rather than as quantitatively demonstrated differences between groups.

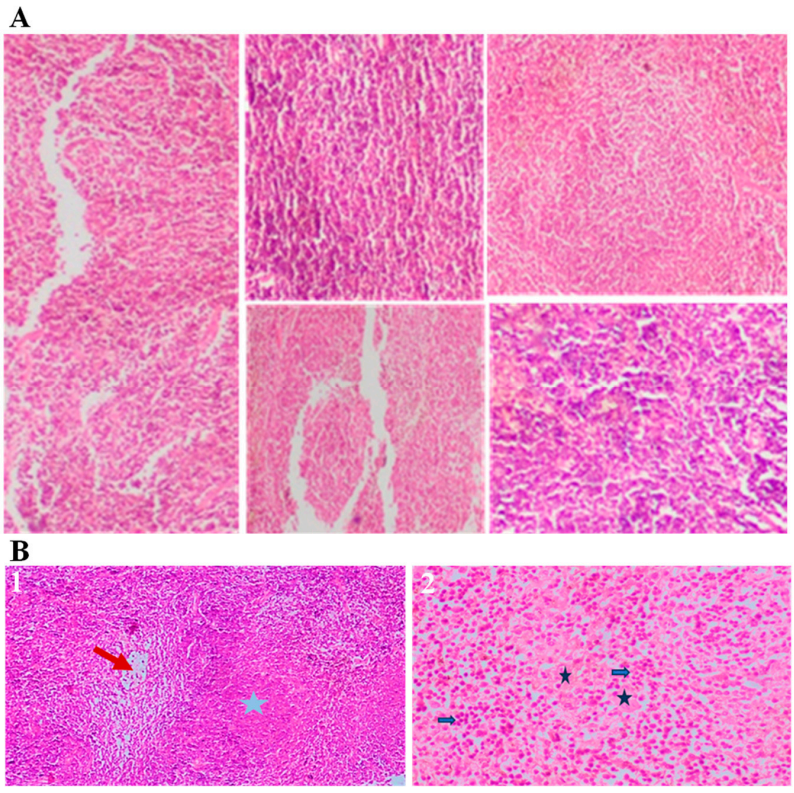


Figure 2. (**A**) Histological images of the normal spleen (10×). (**B**) Histopathological alterations in tissue sections: (**B1**) Focal areas of passive congestion (red arrow) and hemorrhagic necrosis (star) at 10× magnification; (**B2**) Multinucleated giant cells associated with macrophage aggregates (stars) and iron-laden macrophages (siderophages) (arrows) at 40× magnification.

2.2. Antioxidant Activity

Figure 3 depicts the evaluation of *M. charantia*'s antioxidant activity, expressed through IC_{50} values using ABTS and DPPH radical scavenging methods. All tested preparations showed measurable radical-scavenging activity in the ABTS and DPPH assays, likely due to the presence of secondary metabolites in the plant's fruits, leaves, and stems.

Differences between ABTS and DPPH IC_{50} values of *M. charantia* are interpreted as reflecting the distinct physicochemical characteristics of the two cell-free assays.

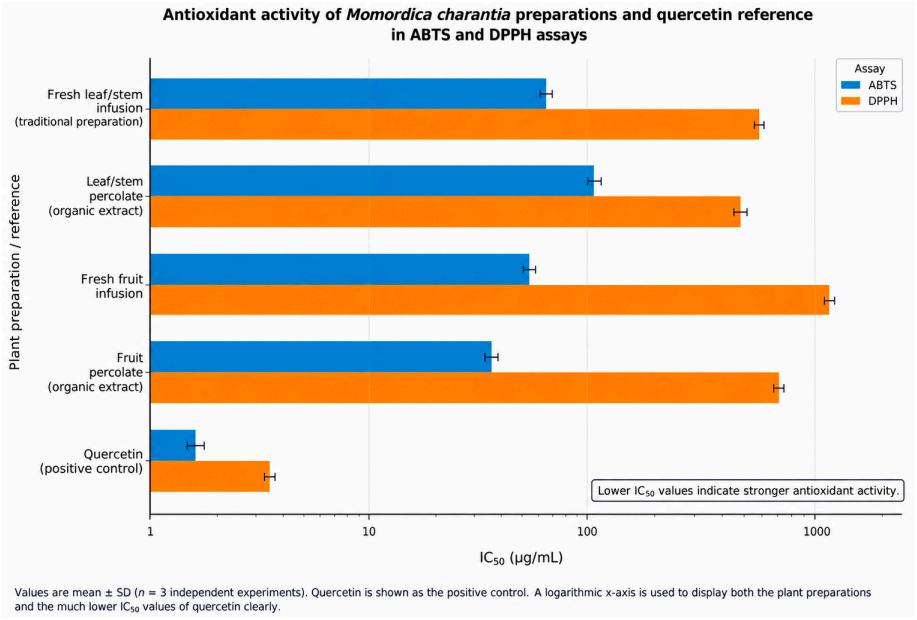


Figure 3. IC_{50} values (µg/mL) of extracts of the leaf-stem mixtures, fruits, and quercetin as a positive control for ABTS and DPPH tests (mean ± standard deviation, $n = 3$).

2.3. Botanical Microscopic Features

Microscopic analysis of *M. charantia* leaf, stem, and fruit powders performed using 2–3 drops of Steinmetz reagent (lactic acid) on glass slides revealed characteristic micrographic elements for each plant organ (Figure 4). In leaf and stem powders (Figure 4A), the following diagnostic elements were identified: annular vessel fragments (1), parenchyma cells (2), fragments of sclerotic fibers and sclérides (3), fibrous tissue (4), spiral vessel fragments (5), and vascular fiber tissue (6). In fruit powder (Figure 4B), the key elements observed were fibers (1), palisade cells (2), fiber fragments (3), epidermis fragments (4), parenchyma cells (5), and sclérides (6).

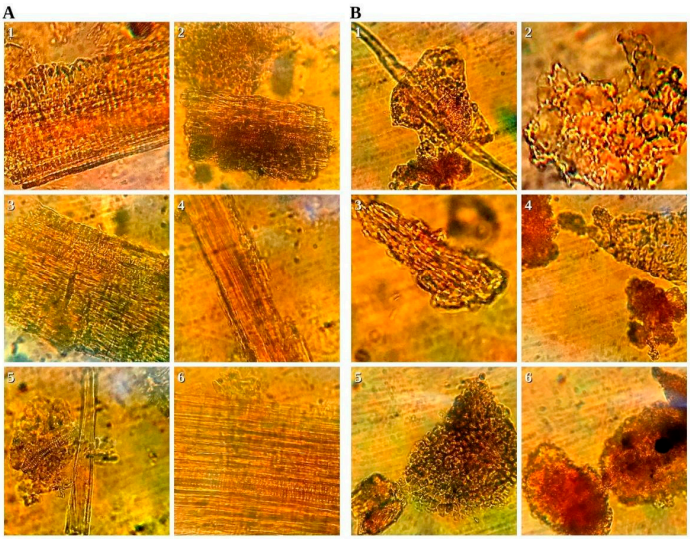


Figure 4. Micrographic features of powdered plant organs of *Momordica charantia*. (**A**) Leaves and stems: annular vessel fragment (**1**); parenchyma cells (**2**); fragments of sclerotic fibers and sclérides (**3**); fibrous tissue (**4**); spiral vessel fragment (**5**); vascular fiber tissue (**6**). (**B**) Fruits: fibers (**1**); palisade cells (**2**); fiber fragments (**3**); epidermis fragments (**4**); parenchyma cells (**5**); sclérides (**6**). Images acquired at 10× and 40× magnification.

2.4. Phytochemical Extract Profiling

2.4.1. UPLC-HRMS Profiling of *M. charantia*

UPLC-HRMS phytochemical analysis of *M. charantia* leaf, stem, and fruit methanolic extracts revealed diverse metabolite features (Figures S5–S7). A selection of ten most intriguing chromatographic features, mainly corresponding to triterpenoids, sterol derivatives, and lipid-related compounds, is shown in Table 4 and Figure 5. Accurate MS (<5 ppm) and AIF MS/MS measurements enabled the assignment of elemental compositions and MS-based tentative annotation from accurate mass and fragmentation patterns (Figures S10–S12).

Table 4. Summary of HRMS-based putatively annotated features detected in methanolic extracts of *M. charantia*.

RT (min)	*m*/*z* [M + H]$^+$	Sum Formula [M]	Structural-Motif Annotation	Part
5.29	437.3411	$C_{30}H_{44}O_2$	Cucurbitane-type triterpenoid isomer	Leaf, Stem, Fruit
6.07	437.3405 [M + Na]$^+$	$C_{28}H_{46}O_2$	Cucurbitane-type triterpenoid isomer	Leaf
6.52	437.3411	$C_{30}H_{44}O_2$	Cucurbitane-type triterpenoid isomer	Leaf, Stem, Fruit
7.65	619.4200	$C_{36}H_{58}O_8$	Glucopyranoside or related triterpenoids	Fruit, Stem
7.95	523.3418	$C_{33}H_{46}O_5$	Cucurbitane-type triterpenoid derivative	Fruit
10.99	282.2787	$C_{18}H_{35}ON$	Fatty amide or isomer	Fruit, Stem
13.33	427.3571	$C_{29}H_{46}O_2$	Phytosterol isomer	Stem, Fruit
14.26	429.3728	$C_{29}H_{48}O_2$	Phytosterol isomer	Fruit, Stem
14.33	613.4845	$C_{39}H_{64}O_5$	Lipidic derivative	Leaf, Stem, Fruit
15.45	429.3726	$C_{29}H_{48}O_2$	Phytosterol isomer	Fruit, leaf

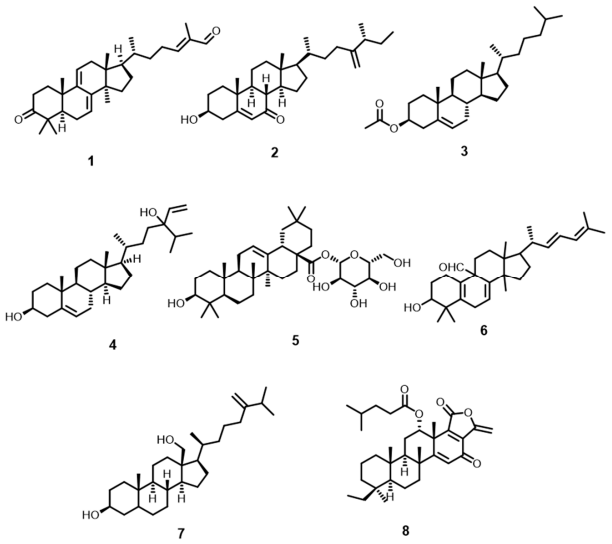


Figure 5. Representative structural motifs associated with selected putative metabolite classes detected in methanolic extracts of *M. charantia*. triterpenoid aldehyde motif (**1**), oxygenated sterol motif (**2**), sterol ester motif (**3**), phytosterol motif (**4**), triterpene-glycoside motif (**5**), cucurbitane-related triterpenoid motif (**6**), oxygenated sterol-like motif (**7**), oxygenated triterpenoid motif (**8**). The depicted structures illustrate natural-product scaffolds based on HRMS annotations and fragmentation patterns.

Several prominent chromatographic features in the methanolic extracts were associated with formulas and fragmentation patterns compatible with triterpenoid- and sterol-related natural products. A recurrent positive-mode feature at *m*/*z* 437.3411 showed fragment ions at *m*/*z* 419, 409, and 391. These data support assignment at the level of a triterpenoid-related structural motif; however, they do not permit unambiguous identification of a unique molecular structure. A second feature detected in leaf extracts at RT 6.07 min showed an ion at *m*/*z* 437.3405, consistent with a sodium-adducted oxygenated sterol- or triterpenoid-

related feature [13,14]. Because structurally distinct compounds may yield similar exact masses and fragmentation pathways, these signals are interpreted conservatively at the formula or chemical-class level.

Additional higher-mass features were consistent with glycosylated triterpenoid-related metabolites, while several late-eluting signals were compatible with sterol- and lipid-related natural-product classes. These observations are consistent with the broad phytochemical diversity previously reported for *M. charantia* [15–19]; however, no individual compound identity, stereochemistry, or specific scaffold was considered definitively established from HRMS data alone. Representative structural motifs illustrating these chemical classes are shown in Figure 5 for chemical context only.

LC-HRMS profiling of aqueous infusions prepared from *M. charantia* leaves, fruits, and stems revealed three recurrent chemical domains: triterpenoid-related features, glycoside-related features, and oxygenated C_{18} lipid-related metabolites (Figures S13–S17). In positive-ion mode, a cluster of signals around *m*/*z* 437.3403–437.3409 was observed in several samples and was considered compatible with dehydrated or otherwise modified triterpenoid-related ions. A second cluster near *m*/*z* 453.336 suggested related, more highly oxygenated features. In negative-ion mode, a series of higher-mass ions, including features around *m*/*z* 633–679, was consistent with glycosylated natural-product motifs previously associated with *M. charantia*. Because these assignments were based primarily on accurate mass and fragmentation behavior, they are presented as class-level annotations rather than definitive identifications.

A further recurrent feature of the aqueous profiles was a series of oxygenated C_{18} lipid-related ions. Signals at *m*/*z* 327.2175–327.2177, 329.2331–329.2333, 311.2226–311.2227, 309.2069–309.2072, 307.1914, 293.2121–293.2123, 313.2385, and 291.1965 formed a coherent group of oxidized lipid-like features across the analyzed organs (Table 5). The ion at *m*/*z* 291.1965 was compatible with an oxo-octadecatrienoic-acid-type motif reported in the phytochemical literature, but the present data can not establish a unique structure. Early-eluting polar features were also observed, including a signal at *m*/*z* 191.0188 compatible with a small organic acid and a feature at *m*/*z* 137.0231 in stem samples; these assignments likewise require confirmation before compound-level identification can be claimed.

Overall, the UPLC-HRMS data indicate that the analyzed *M. charantia* preparations contain chemically diverse features compatible with triterpenoid-, glycoside-, phytosterol-, and oxygenated lipid-related natural-product classes. These mass spectrometry annotations should be regarded as putative. Although the fragmentation patterns provide supportive evidence, they are intended to describe chemical classes and structural motifs rather than definitive compound identities at this level of information. Confirmation of individual structures would require isolation and orthogonal NMR characterization, combined with targeted MS/MS and, where appropriate, comparison with authentic standards.

Table 5. Clustered UPLC-HRMS (Orbitrap) features detected in aqueous infusions of *Momordica charantia* leaves, fruits, and stems, with putative HRMS-based annotations.

Cluster ID	RT Cluster (min)	Observed *m*/*z*	Proposed Ion Type	Proposed Molecular Formula	Putative Chemical Class	Occurrence in Plant Parts (ESI Mode)	Comments
C1	5.82–7.99	437.3403–437.3409	$[M + H–H_2O]^+$	$C_{30}H_{46}O_3$ (neutral, tentative)	Cucurbitane-type triterpenoid aglycone cluster	Leaves (+): 5.82, 6.07, 6.22, 6.44, 6.81, 7.32, 7.99; Fruits (+): 6.22, 6.81, 7.31, 7.98	Strong recurring dehydrated triterpenoid scaffold; highly likely multiple isomers/analogues.
C2	5.17–5.18	453.3358–453.3360	$[M + H–H_2O]^+$ or related $[M + H]^+$ species	$C_{30}H_{46}O_4$ or related (tentative)	More oxygenated cucurbitane-type triterpenoid	Fruits (+) only	Likely related to cluster C1 but more oxygenated; not observed clearly in leaves or stem.
C3	6.05–6.06	663.3756	$[M - H]^-$	$C_{36}H_{56}O_{11}$	Momordicoside-like triterpene glycoside	Leaves (−): 6.05; Fruits (−): 6.05	Shared glycosidic triterpenoid feature in leaves and fruits.
C4	6.06	679.4065–679.4068	$[M - H]^-$	$C_{37}H_{60}O_{11}$	Momordicoside-like triterpene glycoside	Leaves (−): 6.06; Stem (−): 6.06	Strong cross-part glycoside cluster; likely closely related cucurbitane glycoside(s).
C5	6.73–6.81	677.3905	$[M - H]^-$	$C_{37}H_{58}O_{11}$	Oxidized/unsaturated momordicoside-like triterpene glycoside	Leaves (−): 6.73	Likely same triterpene glycoside family as C4, differing by oxidation state/unsaturation.
C6	6.44	633.3648	$[M - H]^-$	$C_{35}H_{54}O_{10}$	Momordicoside-like triterpene glycoside	Leaves (−): 6.44	Related glycoside cluster, observed only in leaves negative mode.
C7	6.57	647.3805	$[M - H]^-$	$C_{36}H_{56}O_{10}$	Momordicoside-like triterpene glycoside	Leaves (−): 6.57	Same glycosidic cucurbitane family; leaf-specific in this dataset.
C8	6.80–6.81	645.3649–645.3651	$[M - H]^-$	$C_{36}H_{54}O_{10}$	Momordicoside-like triterpene glycoside	Leaves (−): 6.81; Fruits (−): 6.80	Shared glycoside cluster between leaves and fruits.
C9	3.73–4.51	327.2175–327.2177	$[M - H]^-$	$C_{18}H_{32}O_5$	Oxylipin-like metabolite/oxygenated C_{18} fatty-acid derivative	Leaves (−): 3.74, 4.51; Fruits (−): 3.73; Stem (−): 3.73	Strong cross-part cluster; likely several chromatographic isomers.
C10	4.35–4.37	329.2331–329.2333	$[M - H]^-$	$C_{18}H_{34}O_5$	Reduced oxylipin-like metabolite/oxygenated C_{18} fatty-acid derivative	Fruits (−): 4.35; Stem (−): 4.36	Shared fruit/stem oxylipin cluster.
C11	5.65	311.2226–311.2227	$[M - H]^-$	$C_{18}H_{32}O_4$	Oxylipin-like metabolite	Fruits (−) only	Part of the fruit oxylipin ladder.

Table 5. *Cont.*

Cluster ID	RT Cluster (min)	Observed *m*/*z*	Proposed Ion Type	Proposed Molecular Formula	Putative Chemical Class	Occurrence in Plant Parts (ESI Mode)	Comments
C12	6.30	309.2069–309.2072	$[M-H]^-$	$C_{18}H_{30}O_4$	Oxylipin-like metabolite	Leaves (−): 6.30; Fruits (−): 6.30	Shared oxygenated C18 cluster between leaves and fruits.
C13	6.44	307.1914	$[M-H]^-$	$C_{18}H_{28}O_4$	More unsaturated/oxidized oxylipin-like metabolite	Fruits (−) only	Chemically coherent with the fruit oxylipin family.
C14	6.06	291.1965	$[M-H]^-$	$C_{18}H_{28}O_3$	Oxo-octadecatrienoic-acid-type metabolite	Fruits (−) only	Best treated as an oxylipin-type feature; likely isomeric possibilities remain unresolved.
C15	7.41–7.43	293.2121–293.2123	$[M-H]^-$	$C_{18}H_{30}O_3$	Oxylipin-like metabolite/oxygenated C_{18} fatty acid	Leaves (−): 7.41; Fruits (−): 7.41; Stem (−): 7.41–7.43	One of the clearest shared cross-part lipid-derived clusters.
C16	7.74	313.2385	$[M-H]^-$	$C_{18}H_{34}O_4$	Reduced oxygenated octadecanoid	Fruits (−) only	Fruit-specific oxylipin-related feature in this dataset.
C17	3.74–7.74	293.2102–293.2107	$[M+H]^+$	$C_{18}H_{28}O_3$ (neutral, tentative)	Positive-mode oxygenated C_{18} metabolite cluster	Leaves (+): 6.31; Fruits (+): 3.74, 5.94, 7.74	Positive-mode counterpart of the C_{18} oxygenated lipid family; likely several isomers.
C18	6.15–7.51	277.2154–277.2159	$[M+H]^+$	$C_{18}H_{28}O_2$ or related (tentative)	Minor apolar oxygenated metabolite cluster	Leaves (+): 7.42; Fruits (+): 6.15, 7.51	Weak but recurrent cross-part minor cluster.
C19	6.66	279.2311	$[M+H]^+$	$C_{18}H_{30}O_2$ or related (tentative)	Minor apolar oxygenated metabolite	Fruits (+) only	Fruit-specific minor feature.
C20	8.20	295.2260	$[M+H]^+$	$C_{18}H_{30}O_3$ or related (tentative)	Minor oxygenated C_{18} metabolite	Fruits (+) only	Likely related to the positive-mode lipid-derived series.
C21	0.63	191.0188	$[M-H]^-$	$C_6H_8O_7$	Citric-acid-related motif	Fruits (−) only	Strong early polar organic acid signal.
C22	1.62	381.1918	$[M-H]^-$	$C_{20}H_{30}O_7$	Unresolved highly oxygenated metabolite	Fruits (−) only	Major early fruit-negative feature; identity unresolved.
C23	2.23	137.0232	$[M-H]^-$	$C_7H_6O_3$	Aromatic hydroxy-acid-type metabolite	Stem (−) only	Consistent with hydroxybenzoic-acid/salicylic-acid-type chemistry, but exact isomer unresolved.

Table 5. *Cont.*

Cluster ID	RT Cluster (min)	Observed *m*/*z*	Proposed Ion Type	Proposed Molecular Formula	Putative Chemical Class	Occurrence in Plant Parts (ESI Mode)	Comments
C24	1.66–1.75	367.0669–367.0671	$[M-H]^-$	Unresolved oxygen-rich metabolite	Early polar oxygen-rich metabolite cluster	Leaves (−): 1.62; Stem (−): 1.66, 1.75	Similar exact-mass region in leaves and stem suggests related highly oxygenated early-eluting metabolites.
C25	7.02	523.3417	$[M+H]^+$ or adduct-related ion	Unresolved; triterpenoid-like region	Unresolved oxygenated triterpenoid-like feature	Leaves (+) only	May belong to a more oxygenated triterpenoid/adduct cluster, but no cross-part match was clear.
C26	9.71	403.2319	$[M+H]^+$	Unresolved	Minor oxygenated terpenoid-like metabolite	Fruits (+) only	Late, isolated, fruit-positive feature.

2.4.2. Thin-Layer Chromatography (TLC) Fingerprinting

The results of the phytochemical screening conducted by TLC highlighted the presence of various bioactive components in the fruits, leaves, and stems. The data are shown in the supporting information: Figure S4A,B.

Phytochemical screening revealed the presence of flavonoids and saponins in fruit extracts, while extracts from leaves and stems contained flavonoids, saponins, and anthraquinones.

2.4.3. Total Flavonoid and Phenol Contents

The flavonoid and total polyphenol contents of *M. charantia* were determined using linear regression equations obtained from calibration curves based on gallic acid and quercetin standards. The corresponding calibration curves are provided in the supplementary materials (Figures S5 and S6).

The results of the quantification are presented in Table 6.

Table 6. Determination of total flavonoid and total polyphenol contents (mean ± standard deviation, $n = 3$).

Plant Part/Solvent Extraction	Total Polyphenols (mg GAE/gDS)	Total Flavonoids (mg QE/g DS)
Leaves and stems	193.690 ± 6.962	72.650 ± 0.580
Fruits	304.820 ± 7.939	26.760 ± 0.584

Legend: mg GAE (gallic acid equivalent) = milligrams of gallic acid equivalents; mg QE (quercetin equivalent) = milligrams of quercetin equivalents; DS = dry sample.

Table 6 shows that the methanolic extract of *M. charantia* fruits exhibited the highest total polyphenol content (304.82 mg GAE/g dry substance) compared to the leaf-stem mixture (193.69 mg GAE/g dry powder). In contrast, the leaf-stem methanolic extract had a higher flavonoid concentration (72.65 mg QE/g dry substance) than the fruit extract (26.76 mg QE/g dry powder).

3. Discussion

A central objective of the present study was to investigate the traditional fresh leaf/stem infusion of *Momordica charantia*, locally used for the management of splenomegaly, and to determine whether the claimed therapeutic relevance of this preparation could be supported experimentally. The additional preparations were included to provide broader pharmacological and phytochemical context and to assess whether the observed activity was specific to the traditional formulation or shared across related preparations. Accordingly, the study combined pharmacological, pharmacognostic, antioxidant, and metabolomic approaches to investigate the medicinal relevance of *M. charantia* in a murine model of cadmium chloride-induced splenic injury. Fresh and dried preparations showed partially overlapping biological and phytochemical characteristics; however, the present study was not designed as a controlled stability comparison, and preservation of the complete phytochemical profile after drying cannot be concluded. Nevertheless, the inclusion of both fresh and processed plant materials remains of practical relevance because dried material is more amenable to storage, transportation, quality control, and future pharmaceutical processing. Dedicated quantitative studies will be required to determine more precisely how drying affects individual metabolites and biological activity.

The splenic alterations observed following cadmium administration are consistent with the known immunotoxic effects of this metal. Cadmium exposure in rodents has previously been associated with splenomegaly, altered splenic architecture, oxidative stress, glutathione depletion, and increased reactive oxygen species production. Pathak and Khandelwal [12],

for example, reported cadmium-induced splenomegaly accompanied by expansion of the red pulp, reduction of the white pulp, and oxidative and apoptotic alterations in splenic cells. These observations support the biological relevance of spleen enlargement as an endpoint in the present model.

The present findings can also be considered in the context of the subsequent study by Pathak and Khandelwal [11], in which piperine attenuated cadmium-induced splenomegaly and the accompanying reduction in body-weight gain. In that study, the response was associated with changes in oxidative and immune parameters. Although piperine and *M. charantia* differ substantially in their chemical composition, this work demonstrates that cadmium-associated splenic alterations can be modified by natural products. It therefore provides a relevant biological context for the present observations without implying that piperine and *M. charantia* act through the same mechanism.

Histopathological examination provided complementary morphological information. Isolated haemorrhagic necrosis was observed at Days 7 and 9, together with passive congestion, siderophage accumulation, macrophage alterations, and occasional multinucleated giant cells in some samples [20]. Given the qualitative nature of the assessment and the absence of a prospectively defined semiquantitative lesion-scoring system, these observations should be interpreted descriptively. The pattern was compatible with more pronounced splenic alterations in the $CdCl_2$-exposed saline disease-control group and comparatively better preservation of splenic architecture in several treated samples, but the available histopathological data do not permit quantitative demonstration of treatment-associated differences.

Of particular importance, the traditional fresh leaf/stem infusion showed the strongest and most consistent Day-9 treatment-associated signal among the tested preparations. Relative and absolute spleen masses were both lower than in the $CdCl_2$-exposed saline disease-control group, and both comparisons met the exploratory Holm-adjusted significance threshold within the Day-9 outcome families. Several other dried extracts showed numerical reductions in absolute spleen mass, but the traditional preparation made of fresh material provided the most coherent combination of effect magnitude, agreement between absolute and relative outcomes, and statistical support. This finding is especially relevant because this formulation corresponds directly to the herbal preparation that motivated the ethnopharmacological investigation. Although the present model cannot validate a clinical curative claim in humans, the results provide experimental support for the biological plausibility of the traditional use and identify the fresh leaf/stem infusion as the priority preparation for further pharmacological investigation.

This observation is also of ethnopharmacological interest. Ahmad et al. [21] reported the traditional use of *M. charantia* in the management of disorders involving the liver and spleen. The Day-9 findings with the traditional fresh leaf/stem infusion therefore provide preliminary experimental support for further investigation of this ethnomedical use. However, cadmium-induced toxic splenic injury is not equivalent to splenomegaly caused by infectious, hematological, or other clinical disorders, and the present findings should not be extrapolated to therapeutic efficacy in humans. Moreover, because administration of the plant preparations began before $CdCl_2$ exposure and continued afterward, the design represents a pretreatment-plus-continuation paradigm rather than therapeutic reversal of established splenic injury.

The observed changes in splenic outcomes are unlikely to arise from a single constituent or pharmacological pathway. *M. charantia* contains numerous chemically and biologically diverse secondary metabolites and has been associated with anti-inflammatory [22], antioxidant [23], antimicrobial [24], antiviral [25], antimalarial [26], and anti-anaemic activities [27]. For example, Mada et al. [24] demonstrated antimicrobial activity of aqueous

and ethanolic leaf extracts against several bacterial species. In the context of cadmium toxicity, oxidative-stress- and inflammation-related pathways are biologically plausible hypotheses; however, they were not directly measured in splenic tissue in the present study and therefore cannot be considered established mechanisms.

The ABTS and DPPH assays provide complementary information on the radical-scavenging properties of the investigated preparations. Differences between the two assays should be interpreted in relation to their distinct reaction environments and radical chemistries. DPPH is commonly used in organic media, whereas the ABTS radical cation can be applied in both aqueous and organic systems. Floegel et al. [28], in a direct comparison of the two assays, found that ABTS and DPPH measurements were correlated but differed in their sensitivity toward individual antioxidant compounds. Accordingly, the differences observed between ABTS and DPPH in the present study are better interpreted as assay-dependent chemical responses rather than contradictory biological effects or evidence that one assay more accurately reflects antioxidant activity.

The measured radical-scavenging activity may be compatible, at least in part, with the presence of phenolic constituents. Polyphenols, including flavonoids, are well established as radical-reactive compounds, and associations between phenolic content and antioxidant activity have frequently been reported [29]. However, no formal correlation analysis was performed here, and the contribution of individual phenolic constituents to the observed assay responses cannot be quantified from the present data. Likewise, the UPLC-HRMS profiles revealed additional triterpenoid-, glycoside-, sterol-, and oxygenated lipid-related features that may be of pharmacological interest, but their contribution to radical-scavenging activity or the in vivo spleen findings was not established.

Comparison with previous studies further illustrates the variability in antioxidant activity reported for *M. charantia*. Pham et al. [30] reported DPPH radical-scavenging activity for an ethyl acetate fruit fraction with an IC_{50} of 0.43 ± 0.04 mg/mL, while ABTS IC_{50} values of 0.36 ± 0.04, 0.35 ± 0.02, and 0.35 ± 0.05 mg/mL were reported for chloroform, ethyl acetate, and n-butanol fractions, respectively. In contrast, Kubola and Siriamornpun [23] reported higher DPPH IC_{50} values for leaf, stem, and fruit extracts. Wu and Ng [31] obtained values closer to those observed in the present investigation, with a methanolic fruit extract showing an IC_{50} of 306.53 µg/mL, while values reported by Rezaeizadeh et al. [32] for methanol/ethyl acetate extracts were of a comparable order of magnitude.

Such differences between studies are expected and should be interpreted cautiously. Antioxidant capacity depends strongly on the plant organ, genotype, geographical provenance, degree of maturity, post-harvest treatment, drying conditions, extraction solvent, extraction efficiency, concentration range, and analytical procedure. Direct ranking of antioxidant activity between studies is therefore inappropriate unless extraction and assay conditions are sufficiently comparable.

Importantly, the in vitro radical-scavenging measurements should not be regarded as direct evidence that radical scavenging is responsible for the in vivo splenic observations. ABTS and DPPH assays measure chemical reactions in cell-free radical systems, whereas antioxidant effects in vivo depend on absorption, metabolism, tissue distribution, intracellular concentrations, and interactions with endogenous defense mechanisms. The parallel observation of radical-scavenging activity and altered splenic outcomes is therefore compatible with, but does not establish, an antioxidant contribution. Unfortunately, no tissue-level oxidative-stress markers, such as malondialdehyde, glutathione, superoxide dismutase, or catalase, were measured. Likewise, inflammatory cytokines, apoptotic markers, and tissue cadmium concentrations were not assessed. Effects on cadmium absorption, redistribution, or chelation therefore cannot be excluded.

The microscopic examination of the plant material provided an additional level of pharmacognostic characterization. The anatomical features observed in the powdered preparations were broadly consistent with previous descriptions of *M. charantia*, although direct comparison is limited because several published studies investigated intact transverse sections rather than powdered material. Poyraz and Derdovski [33], for example, described cuticle, collenchyma, sclerenchyma, cambium, external and internal phloem, xylem, and vascular rays in transverse stem sections. Their examination of leaf sections further revealed upper and lower epidermis, palisade and spongy parenchyma, mesophyll, xylem, phloem, collenchyma, and cystoliths. The fibres, sclerotic fragments, and vascular elements observed in the powdered material in the present study are compatible with these anatomical descriptions and support the pharmacognostic characterization of the examined material. Similarly, the parenchymatous cells and vessel fragments detected in leaf and stem powders are consistent with observations by Shethi et al. [34], who described parenchyma and vascular structures as prominent anatomical features of *M. charantia* leaves. The microscopic appearance of the fruit powder differed to some extent from the intact fruit anatomy reported by Giuliani et al. [35], but such differences are expected because pulverization disrupts the spatial organization of plant tissues. These observations are relevant beyond botanical description because powder microscopy can contribute to pharmacognostic quality control when plant materials have been processed and macroscopic diagnostic features are no longer visible. The characteristics documented here may therefore assist future authentication and quality assessment of *M. charantia* raw materials.

The qualitative phytochemical screening further demonstrated the broad chemical diversity of the investigated material. The results are generally consistent with Fachinan et al. [36], who reported flavonoids, saponins, steroids, anthraquinone-related constituents, triterpenoids, tannins, coumarins, and mucilages in leaf and stem preparations. Akanji et al. [37] and Mada et al. [24] likewise reported several major phytochemical classes, including alkaloids, flavonoids, glycosides, saponins, steroids, and tannins in *M. charantia* leaves. Investigations of the seeds have also reported alkaloids, carbohydrates, glycosides, phytosterols, proteins, flavonoids, tannins, saponins, phenols, and terpenes [35,37–39]. Collectively, these studies support the chemically heterogeneous nature of *M. charantia* observed in the present investigation.

The measured total phenolic content is likewise compatible with the established phytochemical richness of the species, although the comparatively high values observed here require cautious interpretation. Kubola and Siriamornpun [23] demonstrated substantial phenolic content in different anatomical parts of *M. charantia*, and individual phenolic constituents such as caffeic acid and *p*-coumaric acid have been reported [40]. However, quantitative values vary markedly between studies. Wang et al. [41], for example, reported total polyphenol contents of approximately 4.81–6.09 mg GAE/g dry weight in fresh and freeze-dried Chinese and Indian material, whereas Hamissou et al. [42] reported 3.28 mg GAE/g dry weight in fruits. Conversely, Aljohi et al. [43] reported considerably higher values, including 175.33 ± 2.30 mg GAE/g in aqueous fruit extracts and 134.66 ± 1.15 mg GAE/g in pulp extracts. Such variability may result from genotype, geographic origin, climate, maturity, extraction procedure, analytical denominator, and assay methodology [44]. Folin–Ciocalteu measurements may also respond to non-phenolic reducing substances. Consequently, the relatively high values obtained for the Congolese material should not be interpreted as ultimate evidence of a distinct chemotype without analytically matched comparative studies.

The UPLC-HRMS analysis extended the classical phytochemical screening by providing molecular-level information on the chemical diversity of the extracts. Rather than identifying unique compounds unequivocally, the profiles revealed recurrent features compatible with

several broad natural-product classes, including triterpenoid-related, glycoside-related, sterol-related, and oxygenated C_{18} lipid-related metabolites. Representative structural motifs associated with these chemical classes are illustrated in Figure 5, but they should not be interpreted as confirmed molecular identities.

Triterpenoid-related features are particularly relevant in the context of *M. charantia*, because cucurbitane-type natural products are characteristic constituents of the species and numerous members of this family have previously been isolated and structurally characterized [13]. Several signals observed in the present study were compatible with triterpenoid-related structural motifs, including motifs associated in the literature with cucurbitane-type natural products. Their occurrence therefore provides a relevant phytochemical context for the investigated preparations, but the current HRMS evidence does not establish a unique scaffold, stereochemistry, or individual compound identity, nor does it demonstrate a causal contribution to the in vivo observations.

Higher-mass features compatible with glycosylated triterpenoid-related metabolites were also detected. Glycoside-related features occurred across the analyzed plant organs, with some differences in their detection patterns. Such variation is compatible with tissue-dependent phytochemical specialization within *M. charantia*, although the present untargeted profiling was not designed for quantitative comparison of relative metabolite abundance between organs. Organ-specific enrichment or predominance should therefore not be inferred without standardized normalization and quantitative analytical validation.

Sterol- and lipid-related features were also observed and further illustrate the chemical complexity of the extracts. These classes contain numerous constitutional and stereochemical isomers with identical or closely related exact masses and often similar fragmentation behavior. Their interpretation is therefore most appropriately maintained at the chemical-class or structural-motif level unless confirmed by authentic standards or orthogonal structural methods.

Another notable feature of the aqueous profiles was the presence of a series of oxygenated C_{18} lipid-related ions. Their coherent mass distribution and degree of oxygenation were compatible with an oxylipin-like chemical domain. Oxygenated derivatives of polyunsaturated fatty acids are widely involved in plant stress responses, signaling, and defense. Some of the detected features showed exact masses compatible with oxidized C_{18} metabolites previously reported from bitter gourd. Nevertheless, the present HRMS evidence does not establish the precise positions of oxygenation, double-bond geometry, or stereochemistry, and these features should therefore remain described as putative class-level annotations.

From a pharmacological perspective, these triterpenoid-, glycoside-, sterol-, and oxygenated lipid-related features identify chemical classes of potential interest for future biological investigation. However, the present study does not demonstrate that any of these metabolite classes is directly responsible for the observed spleen-mass differences, radical-scavenging activity, or histopathological findings. Targeted fractionation and biological evaluation will be required to establish whether individual metabolites or combinations of metabolites contribute to these effects.

The analyzed plant organs showed both shared and organ-associated chemical features. Such differences are consistent with the metabolic specialization of leaves, stems, and fruits, but the untargeted HRMS data should be interpreted primarily in terms of detected chemical diversity rather than quantitative enrichment. Likewise, although fresh and dried preparations showed partially overlapping phytochemical and biological characteristics, the present work was not designed as a controlled chemical-stability experiment. Quantitative evaluation of the effect of drying would require matched starting material, validated extraction recovery, internal normalization, and targeted analytical measurements.

The HRMS annotations should therefore be interpreted according to established confidence principles for small-molecule identification. High-resolution accurate mass, isotopic distribution, retention behavior, and MS/MS fragmentation can provide evidence for elemental composition, chemical class, or structural motif, but generally cannot establish unequivocal molecular identity for positional or stereochemical isomers. This limitation is particularly relevant for triterpenoids, glycosides, sterol-related constituents, and oxidized lipids, for which numerous natural products may share elemental compositions and related fragmentation pathways. Accordingly, the molecular features reported in the present study are described as putative annotations or class-level assignments where authentic standards were not available. This approach is consistent with the graded identification-confidence framework proposed by Schymanski et al. [45], which emphasizes the distinction between molecular formulas, candidate structures, probable structures, and compounds confirmed with authentic reference materials. Definitive identification of selected metabolites of particular interest would require isolation and orthogonal characterization, including targeted MS/MS, one- and two-dimensional NMR spectroscopy, and, where appropriate, comparison with authentic standards.

Taken together, the chemical data demonstrate that the investigated *M. charantia* preparations contain a complex mixture of natural-product classes rather than a single dominant putative active constituent. This chemical complexity provides several hypotheses for future mechanistic investigation; however, the present data do not establish synergy or the individual contribution of any metabolite class. Oxidative-stress-related mechanisms remain one biologically plausible hypothesis because oxidative injury is implicated in cadmium toxicity, but inflammatory, immunological, toxicokinetic, and metal-binding mechanisms may also contribute and were not directly evaluated.

Thus, the study provides experimental support for further investigation of the traditional fresh leaf/stem preparation of *M. charantia*. Among the tested formulations, this preparation showed the most consistent Day-9 reduction in splenic enlargement, with concordant changes in both absolute and relative spleen mass. The finding is particularly relevant because it directly addresses the ethnopharmacological claim that motivated the study. However, the present results should be regarded as preclinical and hypothesis-generating rather than as validation of a curative effect in human splenomegaly, since cadmium-induced splenic injury does not reproduce the full spectrum of infectious, hematological, or other clinical causes of splenomegaly.

The present study should therefore be interpreted as an exploratory integration of ethnopharmacological context, pharmacognostic characterization, phytochemical profiling, cell-free radical-scavenging assays, qualitative histopathology, and in vivo spleen-mass outcomes. The strongest Day-9 biological signal was observed with the traditional fresh leaf/stem infusion, which showed concordantly lower mean relative and absolute spleen masses than the $CdCl_2$-exposed saline disease-control group. Several other extracts showed numerical reductions in absolute spleen mass, but the statistical evidence was less robust. These observations support further investigation of the traditional preparation rather than establishing therapeutic efficacy or reversal of established splenic injury.

Several limitations should be considered. The study lacked a concurrent non-$CdCl_2$ healthy control, an extract-only control, and an oral vehicle control matched to the plant-treatment groups. Day-1 animals provided pre-exposure information but could not substitute for a concurrent healthy control at Days 7 and 9. Ten unplanned deaths resulted in small and unequal terminal group sizes, and the causes and sex distribution of these deaths were not available. Male and female animals were pooled because the experiment was not powered for sex-stratified analysis. Histopathology was qualitative, tissue cadmium concentrations and tissue-level oxidative, inflammatory, and apoptotic biomarkers were

not determined, and the HRMS/MS annotations remain putative. Furthermore, because the terminal samples were obtained from different animals at each time point, differences between Days 7 and 9 do not represent within-animal recovery or progression.

Future studies should therefore use prospectively defined statistical contrasts, larger and adequately powered groups, concurrent healthy and route-matched vehicle controls, standardized plant preparations, quantitative histopathological scoring, and measurement of tissue cadmium concentrations and relevant oxidative-stress, inflammatory, apoptotic, and immune-cell markers. Bioactivity-guided fractionation and targeted structural characterization of the most relevant metabolite classes may then help distinguish chemical markers from constituents that contribute directly to the biological activity of *M. charantia*.

4. Materials and Methods

4.1. Chemicals and Reagents

All solvents used for HPLC and LC-MS analyses were of analytical grade and purchased from VWR (Leuven, Belgium). 1,1-Diphenyl-2-picrylhydrazyl (DPPH), 2,2′-azino-bis-(3-ethylbenzothiazoline-6-sulfonic acid) (ABTS), 2-aminoethyl diphenylborate, anisaldehyde, and potassium persulfate were purchased from Sigma-Aldrich (Bornem, Belgium). Caffeic acid, chlorogenic acid (purity ≥ 95%), and gallic acid (purity ≥ 97%) were also obtained from Sigma-Aldrich. Rutin (purity ≥ 99%), isoquercetin (purity ≥ 99%), and quercetin (purity ≥ 98.5%) were of HPLC grade and purchased from Extrasynthese (Genay, France). Cadmium chloride monohydrate (purity 98%) and chloroform were obtained from Sigma-Aldrich. Hematoxylin solution (modified according to Gill II) and Eosin Y (0.5% aqueous solution) for histological staining were purchased from E. Merck (Darmstadt, Germany). Canada balsam mounting medium was supplied by Unisource Chemicals (Mumbai, India).

4.2. Material

The leaves, stems, and fruits of *M. charantia* were collected in collaboration with a traditional practitioner in Mikondo, Kinshasa, DRC on 26 October 2022 (Figure 6). The plant was authenticated at the University of Kinshasa Herbarium, where a voucher specimen was digitized and registered under reference number Moke001/2023 (see Supporting Information Figure S1). A portion of the collected plant material was air-dried at room temperature and finely ground into powder using a laboratory grinder for further physicochemical screening and evaluation of its biological activities [46,47]. The remaining fresh material was used to prepare infusions following the traditional practitioner's protocol.



Figure 6. Plant material of *Momordica charantia* collected in Mikondo, Kinshasa, Democratic Republic of Congo. (**A**) Climbing vine showing characteristic lobed leaves, tendrils, and a yellow five-petalled flower. (**B**) Harvested fruits at different stages of maturity, ranging from green to orange at full ripeness, at which point the fruit splits open to expose red-coated seeds.

4.3. Animal Experiments: In Vivo Design

The experimental protocol was adapted from previously published methods [5,11] as described in Figure 7.

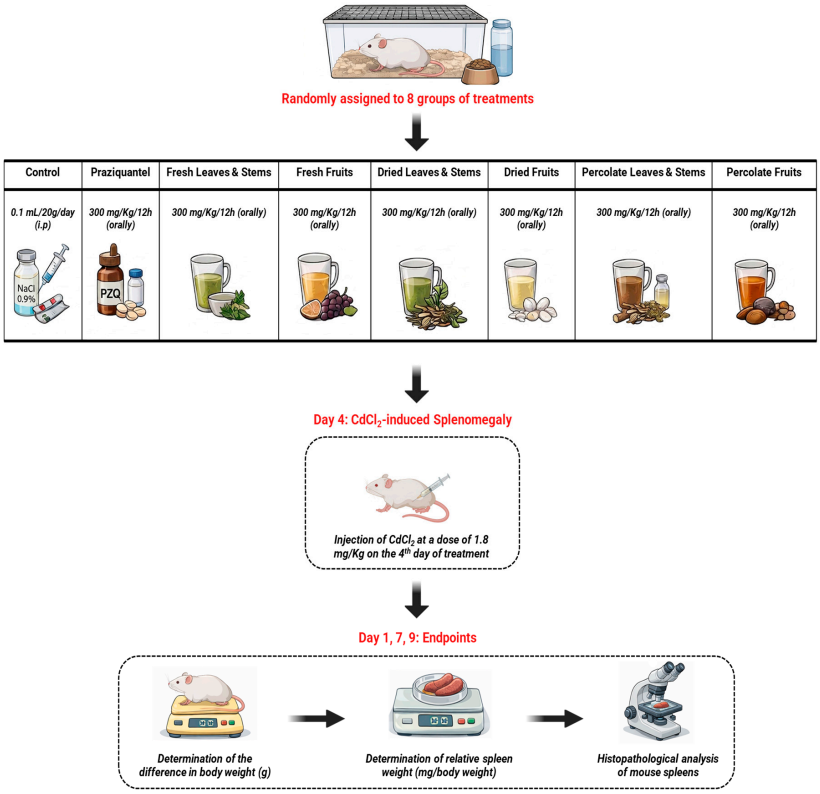


Figure 7. Experimental design for evaluating the in vivo activity of *Momordica charantia* preparation and extracts on $CdCl_2$-induced splenomegaly in mice, and histopathological assessment of mouse spleens for protective effects.

A total of 96 Swiss mice (48 males and 48 females), aged 5–6 weeks and weighing 14–24 g (mean approximately 18.3 g), were enrolled from the *Institut National des Recherches Biomédicales (INRB)*, Kinshasa, Democratic Republic of Congo. The study was conducted under blinded conditions. Personnel administering the treatments were unaware of the identity and composition of the products and of the corresponding treatment allocation. Veterinary monitoring and histopathological assessment were likewise performed blinded to treatment-group allocation and sample identity. Only a designated non-interventional observer had access to the allocation information for documentation purposes and was not involved in treatment administration or outcome assessment. Mice were stratified by body weight to ensure comparable baseline distributions across groups and were then randomly assigned by drawing lots to eight experimental groups (12 animals/group; initially 6 males and 6 females/group). Four animals per group (2 males and 2 females) were scheduled for independent terminal sampling on Days 1, 7 and 9. $CdCl_2$ (1.8 mg/kg, intraperitoneally) was administered once on Day 4. Day 1 therefore represented a pre-exposure terminal sampling point, whereas Days 7 and 9 represented three and five days after $CdCl_2$ exposure, respectively. Because spleen collection was terminal, different animals contributed to the three sampling days, i.e., Day 1, Day 7, and Day 9. Cohorts were therefore considered independent terminal cohorts and not repeated measurements of the same animals. Absolute spleen mass (mg), terminal body mass (g), and relative spleen mass (mg/g body mass; individual spleen mass divided by the corresponding body mass) were reconstructed from the individual-animal records.

The treatment groups were organized as follows. Group I served as the $CdCl_2$-exposed saline disease-control group and received 0.9% NaCl at 0.1 mL/20 g body weight/day by intraperitoneal administration for 9 days. Group II, used as a pharmacological reference-treatment group, received praziquantel at 300 mg/kg every 12 h orally for 9 days. Group III received the traditional preparation consisting of an infusion of fresh *Momordica charantia* leaves and stems at 300 mg dry-extract/kg/day orally for 9 days. Group IV received a fresh-fruit infusion at 300 mg dry-extract/kg/day orally for 9 days. Group V received an infusion of dried leaves and stems at 300 mg dry-extract/kg/day orally for 9 days. Group VI received a dried-fruit infusion at 300 mg dry-extract/kg/day orally for 9 days. Group VII received a leaf/stem percolate at 300 mg dry-extract/kg/day orally for 9 days, and Group VIII received a fruit percolate at 300 mg dry-extract/kg/day orally for 9 days. All groups received a single intraperitoneal injection of $CdCl_2$ (1.8 mg/kg) on Day 4. Accordingly, administration of the plant preparations began before $CdCl_2$ exposure and continued thereafter; the design therefore represents a pretreatment-plus-continuation paradigm rather than therapeutic reversal of established injury. Organic percolates were initially obtained in $MeOH/CH_2Cl_2$, dried at high vacuum to remove traces, before administration in 80% DMSO aqueous solutions. At each scheduled terminal assessment, animals were weighed and placed in a closed chamber, where they were exposed to chloroform until deeply anaesthetized. Animals were monitored throughout the study, and deaths were identified by the absence of spontaneous movement, responsiveness, and other signs of life. Once complete loss of responsiveness was achieved, the veterinarian performed a terminal abdominal procedure and excised the spleen. Absolute spleen mass was recorded in milligrams, and relative spleen mass was calculated as spleen mass divided by the corresponding terminal body mass and expressed as mg/g body weight. Changes in body mass between study entry and terminal assessment were recorded in grams. Excised spleens were immediately fixed in 10% formalin for subsequent histopathological processing [11].

The individual animal was considered the experimental unit. Each experimental group was housed in a separate cage measuring 46 × 27 × 17 cm with a wire-mesh lid. At enrolment, each cage contained 12 mice; following the scheduled Day-1 terminal sampling, up to eight animals remained, and following Day 7, up to four remained, subject to unplanned mortality. Animals had free access to a standardized diet and water and were maintained under artificial room lighting at ambient room temperature. The temperature and relative humidity were not instrumentally recorded. A defined light/dark cycle, bedding and enrichment details, and the acclimatization duration were not documented in the available study records. Animal welfare monitoring included body weight, food intake, water intake, and mobility. Humane endpoint criteria included inability to remain standing, absence of food intake for 24–48 h, and respiratory difficulty.

Male and female animals were pooled for the principal exploratory analysis because the small terminal cohort sizes did not permit adequately powered sex-stratified inference; sex-specific effects therefore cannot be excluded.

For the statistical analysis, one-way ANOVA was used as the omnibus framework for group comparisons within each terminal sampling day. This approach was retained because, within a given sampling day, the treatment group represented the single between-animal experimental factor and observations were independent. A repeated-measures analysis was not appropriate because different animals were sampled terminally on Days 1, 7, and 9. Although a factorial treatment × sampling-day model can be applied to independent cohorts, it was not used as the principal inferential framework because Day 1 preceded $CdCl_2$ exposure and therefore differed biologically from the post-exposure endpoints, while mortality resulted in small and unbalanced post-exposure group sizes.

To further evaluate treatment effects in the presence of unequal sample sizes and to account for multiple testing, the individual-animal data were also analyzed using two-sided Welch comparisons of each treated group, including the pharmacological reference treatment praziquantel, versus the $CdCl_2$-exposed saline disease-control group within Days 7 and 9, separately for absolute and relative spleen mass. Holm-adjusted p values were calculated for the seven treatment contrasts within each day/outcome family. A more conservative sensitivity analysis additionally applied Holm correction across all 28 post-exposure comparisons (seven treatment contrasts × two sampling days × two spleen-mass outcomes).

4.4. Histopathological Analysis

Histopathological processing of formalin-fixed spleen samples was performed following standard protocols adapted from [48,49]. Tissue samples were placed in cassettes and subjected to graded dehydration through six successive immersions in a methanol/isopropanol mixture at 40-min intervals, followed by clearing in three xylene baths (15, 30, and 30 min). Samples were then impregnated with molten paraffin for a minimum of 6 h and embedded in paraffin blocks using standard tissue molds. Sections of 4–5 µm thickness were cut using a rotary microtome and mounted onto glass slides, which were dried at 56–60 °C to ensure optimal tissue adhesion. For hematoxylin and eosin staining, sections were deparaffinized in two xylene baths and rehydrated through graded methanol washes (absolute and 95%), followed by tap water. Sections were stained with hematoxylin for 2–10 min, differentiated in a dilute sulfuric acid/alcohol solution, and blued in lithium carbonate solution for 1 min. Counterstaining with eosin was performed prior to dehydration through three consecutive methanol baths (2–3 min each). Slides were cleared in xylene and coverslipped using Canada balsam as the mounting medium. Stained sections were examined by light microscopy (Olympus CX31RTSF; Tokyo, Japan) at 4×, 10×, and 40× magnification, and representative images were acquired using a Samsung imaging device fitted with an Olympus DP2-SAL adapter (Tokyo, Japan). For histopathological assessment, one male and one female were selected from each group at each scheduled time point from the surviving animals, yielding 48 spleen samples. The deceased animals were not subjected to spleen collection or post-mortem histopathology. The histopathological evaluation was also blinded. The pathology assessment was qualitative rather than based on a prospectively defined semiquantitative lesion-scoring system.

4.5. Ethics and Protocol Approval

The experimental protocol was reviewed and approved by the Comité d'Éthique, École de Santé Publique, Université de Kinshasa, Democratic Republic of the Congo (Approval No. ESP/CE/53B/2024; 3 April 2024), in accordance with the national regulatory framework governed by the *Comité National d'Éthique de la Santé (CNES)*, established under Order No. 1250-ZKM043 of the Ministry of Public Health, Hygiene and Prevention, and the study was conducted in accordance with the ARRIVE guidelines for animal research. Animals were supplied by the accredited animal facility of the *Institut National des Recherches Biomédicales (INRB)*, Kinshasa. The approval considered animal protection and the principles of Replacement, Reduction and Refinement. The protocol was not prospectively registered in a public repository; before experimental work commenced, it was submitted to the INRB laboratory for feasibility review and confirmation that the study could proceed. All procedures were designed to minimize suffering and to keep the number of animals used to the minimum required for statistical validity.

4.6. Microscopic Analysis

Powder observations were made using the European Pharmacopoeia reagent and the lactic acid reagent (Steimetz reagent) [50]. Observations were made using an optical microscope (Novex BBPPH 86.375 microscope, Euromex Microscopen BV., Arnhem, The Netherlands; 10× and 40× magnification), and images were taken using an iPhone 6 Plus.

4.7. Phytochemical Profiling

4.7.1. Sample Preparation

Organic extracts were prepared by percolating 10 g of dried plant powder with 180 mL of dichloromethane/methanol (1:1, *v*/*v*), ethyl acetate, dichloromethane, or methanol individually, following the methods of Elaka et al. [51]. Aqueous extracts were prepared by infusing 100 g of fresh leaves, stems, or crushed fruit with 400 mL of boiling distilled water (100 °C), as described by Ahmed & Adrar [52]. All solvent extracts were dried under reduced pressure using a rotavapor and left in a high-vacuum system for 48–72 h, and the resulting dry extracts were weighed and stored in amber airtight vials at 4 °C until further use. Regarding UPLC-HRMS analysis, 10 mg of dried plant powder was dissolved in 10 mL of methanol (MS grade), sonicated for 5 min, and sequentially filtered through Whatman No. 1 filter paper (Cytiva, Marlborough, MA, USA), followed by a 0.2 µm PTFE membrane filter (Fisher Scientific GmbH, Schwerte, Germany). The aqueous infusions were treated similarly, without the Whatman paper filtration step. The clarified filtrates were further purified by solid-phase extraction using preconditioned Oasis HLB cartridges (Waters Corporation, Milford, MA, USA). An aliquot of 50 µL of the resulting methanolic extract, or infusion, was diluted in 1000 µL of LC-MS grade methanol prior to instrumental analysis. The aqueous infusions analyzed by UPLC-HRMS corresponded to the aqueous preparations used in the biological experiments, whereas the methanolic extracts were prepared separately as laboratory-compatible extracts to broaden phytochemical characterization. They were not intended to represent one-to-one chemical equivalents of the administered aqueous preparations, and the HRMS profiling was exploratory rather than exhaustive.

4.7.2. Liquid Chromatography-Mass Spectrometry (UPLC-HRMS) Analysis

Ultra-Performance Liquid Chromatography-High-Resolution Mass Spectrometry (UPLC-HRMS) analysis was performed using a QExactive Plus Orbitrap mass spectrometer coupled to a Vanquish UPLC system (Thermo Fisher Scientific, Bremen, Germany). A full-scan acquisition method combined with all-ions fragmentation (AIF) and collision-induced dissociation (CID) experiments was used for exploratory metabolite profiling and class-level structural annotation. A volume of 1 µL was always used for injection on the UPLC system operating with an Agilent Eclipse Plus C_{18} column (3.0 × 100 mm, 1.8 µm; Agilent Technologies, Santa Clara, CA, USA) at 60 °C. Chromatographic separation was carried out at a flow rate of 0.4 mL/min using a gradient elution of water containing 0.1% formic acid (eluent A) and acetonitrile containing 0.1% formic acid (eluent B) over a 20-min run. Mass spectrometric detection was performed in both positive and negative electrospray ionization (ESI) modes using nitrogen as the nebulizing and auxiliary gas, under the following conditions: sheath gas flow rate 50, auxiliary gas flow rate 10, spray voltage 4.0 kV, capillary voltage 35 V, capillary temperature 320 °C, and auxiliary gas heater temperature 100 °C. Full-scan spectra were acquired over an m/z range of 100–1500 at a resolution of 75,000 for the profiling of leaf, fruit, and stem infusions, and MS^2 spectra were generated at normalized collision energies of 25 & 30. Data acquisition and processing were carried out using Xcalibur software (version 4.0; Thermo Fisher Scientific, Waltham, MA, USA).

4.7.3. Thin-Layer Chromatography (TLC) Analysis

Analytical TLC of 10 µL of solution at 10 mg/mL of dichloromethane and methanolic extracts was carried out on normal-phase silica gel 60 F_{254} plates (Merck KGaA, Darmstadt, Germany), using different eluents for the identification of secondary metabolites.

4.7.4. Total Flavonoid Analysis

Total flavonoid content was determined in triplicate by UV-VIS spectrophotometer (UV-6300PC; VWR International Europe bvba, Leuven, Belgium) following the method of Mbaiogaou et al. [53], and results are reported as mean values. Blanks were prepared identically, substituting 1 mL of methanol for the extract.

4.7.5. Total Phenol Analysis

Total polyphenol content of the extracts (methanol 80%) was determined using the Folin-Ciocalteu reagent by a UV-VIS spectrophotometric method [53,54]. Total polyphenol content is expressed in mg gallic acid equivalent (GAE)/g dry extract. The preparations were shaken and incubated at room temperature, in the dark, for one hour. Absorbances were measured at 725 nm, and each analysis was performed in triplicate; the average values have been reported.

4.7.6. Cell-Free Antioxidant Assays

The extracts were solubilized in methanol; thus, their effect was compared to a control test performed with methanol alone. Antioxidant activity was assayed through spectrophotometric ABTS and DPPH assays, which were performed according to the method described by Kapepula et al. [55].

4.7.7. Statistical Analysis

The data were subjected to statistical analysis using GraphPad Prism version 8.0.1 (GraphPad Software, San Diego, CA, USA), with a probability threshold of 5% and Python (version 3.15.2) with the SciPy (version 1.18.2) and scikit-learn (version 1.19.1) libraries. For the in vitro analytical assays, measurements were performed in triplicate and are reported as mean ± standard deviation. Values of $p < 0.05$ were considered statistically significant [53].

5. Conclusions

This study provides exploratory experimental support for the traditional fresh leaf/stem infusion of *Momordica charantia*, which constituted the principal ethnopharmacological preparation investigated. Among the tested formulations, this preparation showed the strongest and most consistent Day-9 signal, with lower mean relative and absolute spleen masses than the $CdCl_2$-exposed disease-control group. Several other preparations also showed numerical reductions in absolute spleen mass, but with weaker statistical support. These findings are particularly relevant because they directly address the traditional claim that motivated the study and identify the fresh leaf/stem infusion as the priority preparation for further pharmacological investigation. However, the results do not constitute clinical validation of a curative effect against human splenomegaly. Rather, they provide preclinical evidence of biological activity in a chemically induced model of splenic injury and justify further investigation using adequately powered studies, clinically relevant models, quantitative histopathology, mechanistic biomarkers, and standardized preparations.

Qualitative histopathology suggested partial preservation of splenic architecture in treated animals. UPLC-HRMS profiling revealed features consistent with triterpenoid-, glycoside-, sterol-, and oxygenated lipid-related natural-product classes, while the preparations showed measurable ABTS and DPPH radical-scavenging activity. These findings

support further investigation of the traditional preparation but do not establish therapeutic efficacy, specific active compounds, or a defined mechanism of action. Further studies with matched controls, larger sample sizes, quantitative histopathology, and targeted structural characterization are warranted. Confirmation of these preliminary biological findings will require prospectively designed studies incorporating concurrent healthy controls, larger adequately powered cohorts, and quantitative histopathological scoring, together with appropriate mechanistic and toxicological endpoints.

Supplementary Materials: The following supporting information can be downloaded at: https://www.mdpi.com/article/10.3390/molecules31224183/s1, Table S1: Relative spleen weights; Table S2: Absolute spleen masses after $CdCl_2$ exposure; Table S3: Individual animal-level data used for spleen-mass analyses; Figure S1: Herbarium specimen of *Momordica charantia*; Figures S2–S3: Individual relative and absolute spleen-mass observations; Figure S4: TLC profiles; Figures S5–S6: Gallic acid and quercetin calibration curves; Figures S7–S17: LC-HRMS chromatographic profiles and associated mass spectra of methanolic extracts and aqueous infusions of *M. charantia*.

Author Contributions: D.T.T.: Conceptualization, writing—review & editing, Writing—original draft, Visualization, Validation, Supervision, Resources, Project administration, Methodology, Investigation, Formal analysis, Data curation. J.M.B.: Writing—review & editing, Methodology, Investigation, Data curation. J.M.M.: Writing—review & editing, Writing—original draft, Software, Formal analysis, Data curation. K.K.M.: Writing—review & editing, Software, Investigation, Formal analysis, Data curation. I.E.K.: Writing—review & editing, Data curation, Visualization. P.K.M.: Writing—review & editing, Supervision, Data curation. N.K.N.: Writing—review & editing, Data curation. All authors have read and agreed to the published version of the manuscript.

Funding: This research was funded by the Holger-Pöhlmann Foundation through a small research grant awarded to J.M.B at the University of Kinshasa in 2023.

Institutional Review Board Statement: The animal study protocol was approved by the Comité d'Éthique, École de Santé Publique, Université de Kinshasa, Democratic Republic of the Congo (protocol code ESP/CE/53B/2024; approved on 3 April 2024).

Informed Consent Statement: Not applicable.

Data Availability Statement: All data generated or analyzed during this study are included in this published article and its Supporting Information.

Acknowledgments: The authors express their gratitude to Pauline Mufiniki, a traditional healer, for her collaboration, and Landu from the University of Kinshasa for his expertise in plant identification. Special thanks to Gaby Moke, anatomy and pathology laboratory technician at the Faculty of Medicine, for processing the spleen samples, and Bienvenu Lebwaze Massamba from the anatomy and pathology department for conducting the histopathological analysis and excellent service.

Conflicts of Interest: Author Dieudonné Tshitenge Tshitenge was employed by Crop Protection, Research & Development, Crop Science Division, Bayer AG, 40789 Monheim am Rhein, Germany. The remaining authors declare that the research was conducted in the absence of any commercial or financial relationships that could be construed as a potential conflict of interest.

Dedication: This work is dedicated to Professor Emeritus Dibungi Kalenda Tshimbombo, University of Kinshasa, in recognition of his outstanding contribution to training and mentorship of a new generation of scientists in pharmacognosy and analytical chemistry.

References

1. Fatima, E.H.; Akka, B.; Dahmani, J.; Belahbib, N.; Zidane, L. Étude Ethnobotanique des Plantes Médicinales Utilisées dans le Traitement des Infections du Système Respiratoire dans le Plateau Central Marocain. *J. Anim. Plant Sci.* **2015**, *25*, 3886–3897.
2. Zhai, Y.; Zhao, Y.; Zhang, Y.; He, J.; Tang, M.; Liu, Y.; Yang, G.; Xue, P.; Yao, Y.; He, M.; et al. Lead suppresses interferon γ to induce splenomegaly via modification on splenic endothelial cells and lymphoid tissue organizer cells in mice. *Ecotoxicol. Environ. Saf.* **2022**, *244*, 114046. [CrossRef]

3. Pozo, A.L.; Godfrey, E.M.; Bowles, K.M. Splenomegaly: Investigation, diagnosis and management. *Blood Rev.* **2009**, *23*, 105–111. [CrossRef]
4. Leblond, V. Journal des Femmes Santé. Splénomégalie: Cause, taille de la rate, symptômes, traitement. 2014. Available online: https://sante.journaldesfemmes.fr/fiches-maladies/2659187-splenomegalie-cause-taille-de-la-rate-symptomes-traitement/ (accessed on 3 November 2026).
5. Kong, D.; Zhou, C.; Guo, H.; Wang, W.; Qiu, J.; Liu, X.; Liu, J.; Wang, L.; Wang, Y. Praziquantel targets M1 macrophages and ameliorates splenomegaly in chronic schistosomiasis. *Antimicrob. Agents Chemother.* **2018**, *62*, e00005-17. [CrossRef]
6. de la Pinta, C.; Lizarbe, E.F.; Luis, Á.M.; Rullán, J.A.D.; García, S.S. Treatment of symptomatic splenomegaly with low doses of radiotherapy: Retrospective analysis and review of the literature. *Tech. Innov. Patient Support Radiat. Oncol.* **2017**, *3–4*, 23–29. [CrossRef]
7. Mesa, R.A. How I treat symptomatic splenomegaly in patients with myelofibrosis. *Blood* **2009**, *113*, 5394–5400. [CrossRef]
8. Chanda, R.; Samadder, A.; Banerjee, J. Anti-diabetic Activity of *Momordica charantia* or Bitter Melon: A Review. *Acta Sci. Pharm. Sci.* **2019**, *3*, 24–30.
9. Husna, R.N.; Noriham, A.; Nooraain, H.; Azizah, A.H.; Amna, O.F. Acute Oral Toxicity Effects of *Momordica charantia* Sprague Dawley Rats. *Int. J. Biosci. Biochem. Bioinform.* **2013**, *3*, 4–6. [CrossRef]
10. Osadolor Bini, N.; And, H.B.; Elekofehinti, O.O. Protective Potential of *Momordica charantia* against CCl4 Induced Change in Liver and Kidney Serum Biomarkers in Wistar Rats. *Sokoto J. Med. Lab. Sci.* **2024**, *9*, 301–307. [CrossRef]
11. Pathak, N.; Khandelwal, S. Immunomodulatory role of piperine in cadmium induced thymic atrophy and splenomegaly in mice. *Environ. Toxicol. Pharmacol.* **2009**, *28*, 52–60. [CrossRef]
12. Pathak, N.; Khandelwal, S. Role of oxidative stress and apoptosis in cadmium induced thymic atrophy and splenomegaly in mice. *Toxicol. Lett.* **2007**, *169*, 95–108. [CrossRef]
13. Kimura, Y.; Akihisa, T.; Yuasa, N.; Ukiya, M.; Suzuki, T.; Toriyama, M.; Motohashi, S.; Tokuda, H. Cucurbitane-type triterpenoids from the fruit of *Momordica charantia*. *J. Nat. Prod.* **2005**, *68*, 807–809. [CrossRef]
14. Xu, T.; Zhao, Q.M.; Yao, L.G.; Lan, L.F.; Li, S.W.; Guo, Y.W. Sinulasterols D–G, four new antibacterial steroids from the South China sea soft coral Sinularia depressa. *Steroids* **2023**, *192*, 109182. [CrossRef]
15. Mahato, S.B.; Kundu, A.P. 13C NMR Spectra of pentacyclic triterpenoids-a compilation and some salient features. *Phytochemistry* **1994**, *37*, 1517–1575. [CrossRef]
16. Sawzik, P.; Craven, B.M. The crystal structure of 1,2-dipalmitoyl-sn-glycerol at 123 K. *Chem. Phys. Lipids* **1979**, *71*, 219–228. [CrossRef]
17. Weber, H.-P.; Craven, B.M.; Sawzik, P.; McMullan, R.K. Crystal structure and thermal vibrations of cholesteryl acetate from neutron diffraction at 123 and 20 K. *Acta Crystallogr. Sect. B* **1991**, *47*, 116–127. [CrossRef]
18. Cravatt, B.F.; Prospero-Garcia, O.; Siuzdak, G.; Gilula, N.B.; Henriksen, S.J.; Boger, D.L.; Lerner, R.A. Chemical Characterization of a Family of Brain Lipids That Induce Sleep. *Science* **1995**, *268*, 1506–1509. [CrossRef]
19. Zhang, H.J.; Yi, Y.H.; Yang, F.; Chen, W.S.; Lin, H.W. Sesterterpenes and a new sterol from the marine sponge Phyllospongia foliascens. *Molecules* **2010**, *15*, 834–841. [CrossRef]
20. Lombard, V.; Brabois, R. Pathologies Spléniques, 2012. Available online: https://onclepaul.net/wp-content/uploads/2011/07/Pathologies-spl%C3%A9niques-DU-VLo-2012FILEminimizer.pdf (accessed on 3 November 2026).
21. Ahmad, N.; Hasan, N.; Ahmad, Z.; Zishan, M.; Zohrameena, S. *Momordica charantia*: For traditional uses and pharmacological actions. *J. Drug Deliv. Ther.* **2016**, *6*, 40. [CrossRef]
22. Chao, C.Y.; Sung, P.J.; Wang, W.H.; Kuo, Y.H. Anti-inflammatory effect of *Momordica charantia* in sepsis mice. *Molecules* **2014**, *19*, 12777–12788. [CrossRef]
23. Kubola, J.; Siriamornpun, S. Phenolic contents and antioxidant activities of bitter gourd (*Momordica charantia* L.) leaf, stem and fruit fraction extracts in vitro. *Food Chem.* **2008**, *110*, 881–890. [CrossRef]
24. Mada, S.B.; Garba, A.; Mohammed, H.A.; Muhammad, A.; Olagunju, A. Antimicrobial activity and phytochemical screening of aqueous and ethanol extracts of *Momordica charantia* L. leaves. *J. Med. Plants Res.* **2013**, *7*, 579–586. [CrossRef]
25. Au, T.K.; Collins, R.A.; Lam, T.L.; Ng, T.B.; Fong, W.P.; Wan, D.C.C. The plant ribosome inactivating proteins luffin and saporin are potent inhibitors of HIV-1 integrase. *FEBS Lett.* **2000**, *471*, 169–172. [CrossRef]
26. Ali, M.H.; Ibrahim, I.; Jasamai, M.; Embi, N.; Sidek, H. Anti-malarial Effect of *Momordica charantia* Involved Modulation of Cytokine Mediated via GSK3β Inhibition in Plasmodium berghei- Infected Mice. *Jordan J. Biol. Sci.* **2022**, *15*, 523–529. [CrossRef]
27. Sandeep, D.; Vidyadhara, S.; Srinivasulu, P. Comparative anti-anaemic activity of methanolic extracts of *Momordica charantia* and Luffa acutangula. *Curr. Trends Biotechnol. Pharm.* **2022**, *16*, 155–161.
28. Floegel, A.; Kim, D.; Chung, S.; Koo, S.I.; Chun, O.K. Comparison of ABTS/DPPH assays to measure antioxidant capacity in popular antioxidant-rich US foods §. *J. Food Compos. Anal.* **2011**, *24*, 1043–1048. [CrossRef]
29. Bidie, A.P.; N'guessan, B.B.; Yapo, A.F.; N'Guessan, J.D.; Djaman, A.J. Activités antioxydantes de dix plantes medicinales de la pharmacopée ivoirienne. *Sci. Nat.* **2011**, *8*, 1–11.

30. Pham, T.M.H.; Ngo, D.-H.; Vo, T.S. Investigation of Biological Activities of Wild Bitter. *Biomolecules* **2019**, *9*, 211. [CrossRef]
31. Wu, S.; Ng, L. Antioxidant and free radical scavenging activities of wild bitter melon (*Momordica charantia* Linn. var. abbreviata Ser.) in Taiwan. *LWT* **2008**, *41*, 323–330. [CrossRef]
32. Rezaeizadeh, A.; Zuki, A.B.Z.; Abdollahi, M.; Goh, Y.M.; Noordin, M.M.; Hamid, M.; Azmi, T.I. Determination of antioxidant activity in methanolic and chloroformic extracts of *Momordica charantia*. *Afr. J. Biotechnol.* **2011**, *10*, 4932–4940. [CrossRef]
33. Poyraz, İ.E.; Derdovski, C. Morpho-anatomical investigations on *Momordica charantia* L. (Cucurbitaceae). *Anadolu Univ. J. Sci. Technol. –C Life Sci. Biotechnol.* **2016**, *5*, 23–30. [CrossRef]
34. Shethi, K.J.; Doty, M.K.; Liza, S.J.; Rashid, P. Anatomical study of *Momordica charantia* L. from Bangladesh. *Dhaka Univ. J. Biol. Sci.* **2018**, *27*, 69–74. [CrossRef]
35. Giuliani, C.; Tani, C.; Bini, L.M. Micromorphology and anatomy of fruits and seeds of bitter melon (*Momordica charantia* L., Cucurbitaceae). *Acta Soc. Bot. Pol.* **2016**, *85*, 1–7. [CrossRef]
36. Fachinan, R.; Fagninou, A.; Nekoua, M.P.; Amoussa, A.M.; Adjagba, M.; Lagnika, L.; Lalèyè, A.; Moutairou, K.; Yessoufou, A. Evidence of immunosuppressive and Th2 immune polarizing effects of antidiabetic *Momordica charantia* fruit juice. *BioMed Res. Int.* **2017**, *2017*, 9478048. [CrossRef]
37. Akanji, O.C.; Olutayo, C.M.C.; Elufioye, O.T.; Ogunsusi, O.O. The antimalaria effect of *Momordica charantia* L. and *Mirabilis jalapa* leaf extracts using animal model. *J. Med. Plants Res.* **2016**, *10*, 344–350. [CrossRef]
38. Costa, J.G.M.; Nascimento, E.M.M.; Campos, A.R.; Rodrigues, F.F.G. Antibacterial activity of *Momordica charantia* (Curcubitaceae) extracts and fractions. *J. Basic Clin. Pharm.* **2011**, *2*, 45–51.
39. Zahan, S.; Uddin, S.N.; Hossain, M.K.; Mannan, A.B.; Rahman, M.; Chen, U.; Mazumder, T.; Uddin, A.M.; Arefin, S.; Hussain, M.S. Evaluation of phytochemical and pharmacological properties of seeds of *Momordica charantia*. *Avicenna J. Phytomed.* **2020**, *10*, 448–459.
40. Gao, H.; Wen, J.-J.; Hu, J.-L.; Nie, Q.-X.; Chen, H.-H.; Nie, S.-P.; Xiong, T.; Xie, M.-Y. *Momordica charantia* juice with *Lactobacillus plantarum* fermentation: Chemical composition, antioxidant properties and aroma profile. *Food Biosci.* **2018**, *29*, 62–72. [CrossRef]
41. Wang, L.; Clardy, A.; Hui, D.; Gao, A.; Wu, Y. Antioxidant and antidiabetic properties of Chinese and Indian bitter melons (*Momordica charantia* L.). *Food Biosci.* **2019**, *29*, 73–80. [CrossRef]
42. Hamissou, M.; Smith, A.C.; Carter, R.E.; Triplett, J.K. Antioxidative properties of bitter gourd (*Momordica charantia*) and zucchini (*Cucurbita pepo*). *Emir. J. Food Agric.* **2013**, *25*, 641–647. [CrossRef]
43. Aljohi, A.; Matou-Nasri, S.; Ahmed, N. Antiglycation and antioxidant properties of *Momordica charantia*. *PLoS ONE* **2016**, *11*, 1–14. [CrossRef]
44. Aminah, A.; Anna, P.K. Influence of ripening stages on physicochemical characteristics and antioxidant properties of bitter gourd (*Momordica charantia*). *Int. Food Res. J.* **2011**, *18*, 895–900.
45. Schymanski, E.L.; Jeon, J.; Gulde, R.; Fenner, K.; Ruff, M.; Singer, H.P.; Hollender, J. Identifying small molecules via high resolution mass spectrometry: Communicating confidence. *Environ. Sci. Technol.* **2014**, *48*, 2097–2098. [CrossRef]
46. Boulou, G.E.K.; Attiqoua, B.; G'guessan, A.C.; Coulibaly, A.; N'guessan, J.D.; Djaman, A.J. Évaluation in vitro de l'activité antibactérienne des extraits de *Terminalia glaucescens* planch. sur *Salmonella typhi* et *Salmonella typhimurium*. *Bull. La Société R. Des. Sci. Liège* **2011**, *80*, 772–790.
47. Fernandes, N.P.C.; Lagishetty, C.V.; Panda, V.S.; Naik, S.R. An experimental evaluation of the antidiabetic and antilipidemic properties of a standardized *Momordica charantia* fruit extract. *BMC Complement. Altern. Med.* **2007**, *7*, 29. [CrossRef]
48. Luna, L.G. *Manual of Histologic Staining Methods of the Armed Forces Institute of Pathology*, 3rd ed.; Blakiston Division, McGraw-Hill: New York, New York, USA, 1968.
49. Bouchard, D.; Chalifoux, M.; Gaboury, L.; Houde, B.; Laliberté, C.; Martel, A.-M.; Sénécal, J.; Tremblay, C. *Guide d'anatomopathologie*; Ordre professionnel des technologistes médicaux du Québec (OPTMQ): Montréal, QC, Canada, 2014; ISBN 978-2-9814023-3-2.
50. Bahati, L.M.; Kapepula, P.M.; Kabamba, N.N.; Moni, B.; Kafuti, G.M.; Mungitshi, P.M.; Pambu, A.; Bongo, G.; Mukuta, A.T.; Kabengele, J.K.; et al. Microscopic Features, Chromatographic Fingerprints and Antioxidant Property of Some Unconventional Green Leafy Vegetables Consumed in Bandundu, DR Congo. *Pharmacogn. Commun.* **2017**, *7*, 158–163. [CrossRef]
51. Elaka, I.K.; Kapepula, P.M.; Ngombe, N.K.; Mpoyi, J.M.; Lukusa, D.M.; Muabilwa, M.M.; Gbha'Bey, C.K.; Lukukula, C.M.; Lukebakio, B.N.; Okuna, M.K.; et al. Microscopic Features, Antioxidant and Antibacterial Capacities of Plants of the Congolese Cosmetopoeia. *Raw Mater. Cosmeceuticals* **2020**, *8*, 149–166.
52. El-Kheir, A.O.; Naima, A.; Siham, N. Le pouvoir antibactérien de l'extrait infusé de Cistanche tinctoria sur quelques souches bactériennes. Master's Thesis, Université Ahmed Draïa, Faculté des Sciences et de la Technologie, Département des Sciences de la Nature et de la Vie, Adrar, Algeria, 2022. Available online: https://bucket.theses-algerie.com/files/repositories-dz/4997241952562925.pdf? (accessed on 3 November 2026).
53. Mbaiogaou, A.; Betoloum, S.M.; Mbaihougadobe, S.; Naitormbaide, M.; Sale, S.; Mahmout, Y. Determination of phenolic compound contents in fruits of *Momordica charantia* L. (Cucurbitaceae) from Chad. *Int. J. Biol. Chem. Sci.* **2022**, *16*, 1475–1483. [CrossRef]

54. Quettier-Deleu, C.; Gressier, B.; Vasseur, J.; Dine, T.; Brunet, C.; Luyckx, M.; Cazin, M.; Cazin, J.-C.; Bailleul, F.; Trotin, F. Phenolic compounds and antioxidant activities of buckwheat (*Fagopyrum esculentum* Moench) hulls and flour. *J. Ethnopharmacol.* **2000**, *72*, 35–42. [CrossRef]
55. Kapepula, P.M.; Tshala-Katumbay, D.; Mumba, D.; Frédérich, M.; Mbemba, T.; Ngombe, N.K. Traditional Foods as Putative Sources of Antioxidants with Health Benefits in Konzo. In *Antioxidants in Foods and Its Applications*; Shalaby, E., Azzam, G.M., Eds.; IntechOpen: London, UK, 2018; pp. 117–135.

Disclaimer/Publisher's Note: The statements, opinions and data contained in all publications are solely those of the individual author(s) and contributor(s) and not of MDPI and/or the editor(s). MDPI and/or the editor(s) disclaim responsibility for any injury to people or property resulting from any ideas, methods, instructions or products referred to in the content.